Synthetic Metals 230 (2017) 73–78

Contents lists available at ScienceDirect

Synthetic Metals

journal homepage: www.elsevier.com/locate/synmet

Improved device performance stability of bulk-heterojunction hybrid solar cells with low molecular weight PCPDPTB

Alfian F. Madsuha[a,b], Michael Krueger[c,*]

[a] Freiburg Materials Research Centre, University of Freiburg, Stefan-Meier Str. 21, 79104 Freiburg, Germany
[b] Institute of Microsystems Technology (IMTEK), University of Freiburg, George Koehler Allee 103, D-79110 Freiburg, Germany
[c] Carl-von-Ossietzky University Oldenburg, Institute of Physics, Carl-von-Ossietzky Str. 9-11, D-26129 Oldenburg, Germany

ARTICLE INFO

Keywords:
CdSe quantum dots
Molecular weight
PCPDTBT
Hybrid solar cells
Device stability

ABSTRACT

The molecular weight effect of low band-gap conjugated polymer, poly[2,6-(4,4-bis-(2-ethylhexyl)-4H-cyclopenta[2,1-*b*;3,4-*b*′]dithiophene)-alt-4,7-(2,1,3-benzothiadiazole)], PCPDTBT, with an optical energy gap of Eg ~1.4 eV, on the device stability of quantum dot polymer hybrid solar cells has been studied. The PCPDTBT is integrated into hybrid polymer/QDs solar cells, where PCPDTBT acts as electron donor and CdSe QDs as electron acceptor. Morphology investigation and results on device performance over time indicate that low molecular weight PCPDTBT is preferable to fabricate high efficiency hybrid solar cells with long-term stability. An average power conversion efficiency of 2% was measured for PCPDTBT-CdSe QD devices with a molecular weight of < 12 kDa. The long-term stability of the photovoltaic performance of the devices was investigated and found superior compared to devices with PCPDTBT of higher molecular weight. About 96% of the PCE remained after a week of storage of solar cell devices without any further encapsulation in a glove-box. It is assumed that the improvement is mainly due to the better distribution of CdSe QDs within the polymer matrix of low molecular weight PCPDTBT in hybrid solar cells and an improved preservation of the nanomorphology of the hybrid film over time.

1. Introduction

The polymer poly[2,6-(4,4-bis-(2-ethylhexyl)-4H-cyclopenta[2,1-*b*;3,4-*b*′]dithiophene)-alt-4,7-(2,1,3-benzothiadiazole)] (PCPDTBT) recently developed as a state-of-the-art electron donating organic semiconductor for application in organic solar cells (OSCs) and hybrid solar cells (HSCs) [1,2]. For instance, when blended with the fullerene derivative of $PC_{71}BM$ in a bulk-heterojunction (BHJ) architecture, power conversion efficiencies (PCEs) above 6% have been achieved with open-circuit voltages (V_{OC}) in the range of 0.9 V [3]. Whereas, in hybrid solar cells, recently efficiencies of 4% have been reported when combined with CdSe QDs [4]. Although other alternative low bandgap polymers have been demonstrated to lead to higher PCEs [5] in recent years, the interest in PCPDTBT remains high due to its thermal stability, ease of processability as well as commercial availability. Moreover, a deep highest occupied molecular orbit (HOMO) level of PCPDPTBT leads to a reduced susceptibility to oxidation when compared to polymers Poly ({4,8-bis[(2-ethylhexyl)oxy]benzo[1,2-b:4,5-b′]dithiophene-2,6-diyl} {3-fluoro-2-[(2-ethylhexyl)carbonyl]thieno[3,4-*b*]thiophenediyl}) like PTB7, which suffer from rapid photo-oxidative damage [6]. Such features drove PCPDTBT to become the most reliable polymer for photoactive layers in hybrid solar cell applications in recent years.

The nanoscale morphology of the active layer is a crucial parameter for the device performance of hybrid solar cells [7–9]. The main parameters that influence the device performance of BHJ hybrid solar cells are: (i) the composition of the blended solution, (ii) surface modification of nanocrystals (iii) the drying conditions during the formation of the active layer. The importance of the nanomorphology of the photoactive film in hybrid solar cells have garnered attention within the research community which resulted in a huge number of published reviews and reports [2,10–17]. However, it is essential to investigate PCPDTBT itself, which plays a fundamental role as it is used as donor for hybrid solar cell and also affects the morphology of the photoactive layer. The molecular weight of donor polymers have been shown to affect the performance of OSCs, particularly for P3HT:PCBM blends. Ballantyne et al. [18], have reported that the hole mobility was relatively constant between 13 kDa–18 kDa (1 Da = 1.66×10^{-27} kg) and then dropped by an order of magnitude as the molecular weight increased. The measured drop in hole mobility was accompanied by a change in surface morphology and leads to a decreased fill factor of photovoltaic devices. Furthermore, Ma et al. [19] concluded that the choice of optimum annealing temperature for P3HT:PCBM blends is

* Corresponding author.
E-mail addresses: alfian.madsuha@saturn.uni-freiburg.de (A.F. Madsuha), michael.krueger@uni-oldenburg.de (M. Krueger).

http://dx.doi.org/10.1016/j.synthmet.2017.05.018
Received 16 December 2016; Received in revised form 24 May 2017; Accepted 29 May 2017
0379-6779/ © 2017 Elsevier B.V. All rights reserved.

Table 1
Summary of PCPDTBT specifications.

PCPDTBT	Moleculer weight[a] (GPC)	Polydispersity index (PDI)	Purity
P12K	< 12 kDa	2.4	99.99%
P35K	> 35 kDa	< 3.0	99.99%

[a] Determined by GPC against polystyrene standards.

also depended on the molecular weight of the P3HT. These studies indicate the importance of molecular weight on the optimization of OSCs efficiency. Many reports have been displayed with varying values for optimum molecular weight due to discrepancies behavior; however most of them are applied in organic PCBM system, and no investigations in hybrid system have been reported as far as we know. Therefore, the effect of molecular weight (Mw) of conjugated polymer PCPDPDT incorporated into hybrid solar is investigated and correlated to device performance.

We studied PCPDTBT:CdSe QDs BHJ blend thin films with two different molecular weights of PCPDTBT. PCPDTBT with different molecular weight were purchased from 1-Material; and coded as P12K and P35K, representing their molecular weight, $< 12000\ g\ mol^{-1}$ (low Mw) and $> 35000\ g\ mol^{-1}$ (high Mw) respectively. A summary of the specifications of the polymers is listed in Table 1.

The PCPDTBT polymers were blended with CdSe QDs to form photoactive layers utilized in hybrid solar cell devices. It was found that the molecular weight of PCPDTBT affects the device performance of CdSe QDs hybrid solar cell devices. Investigation of the relationship between Mw and device performance can help to choose the right conjugated polymer material for fabricating efficient HSCs devices.

2. Experimental

2.1. CdSe QDs synthesis

Highly crystalline CdSe QDs with an average diameter of about 6.5 nm were synthesized by a hot-injection method, according to the procedure reported in Ref [20,21]. Before being incorporated into polymer, CdSe QDs were washed by a post-synthetic hexanoic acid treatment. The detailed washing procedure has been reported in Ref [15]. Afterwards CdSe QDs were dissolved in chlorobenzene (CB) establishing a concentration of 20 mg/mL.

2.2. Polymer–CdSe QDs hybrid material formation

A photoactive ink was formed by mixing CdSe QDs solution with the PCPDTBT polymer solution. PCPDTBT polymer with two different molecular weights, 12 kDa and 35 kDa, were purchased from 1-Material and dissolved in chlorobenzene to reach as well a concentration of 20 mg/mL. CdSe QDs solution was mixed with PCPDTBT solution with 86:14 wt ratio.

2.3. Solar cell device fabrication

The devices were fabricated on a structured ≤10 Ωsq ITO substrate from Präzisions Glas & Optik GmbH. After 5 min treatment with oxygen plasma, PEDOT:PSS from Baytron AI4083 HC Starck was spin coated on top, resulting into a ~70 nm thick hole transport layer. Afterwards, the photoactive ink was spin coated using a WS400-6NPP-Lite spin coater from Laurell Technologies at 1100 rpm for 30 s, followed by a 1 min

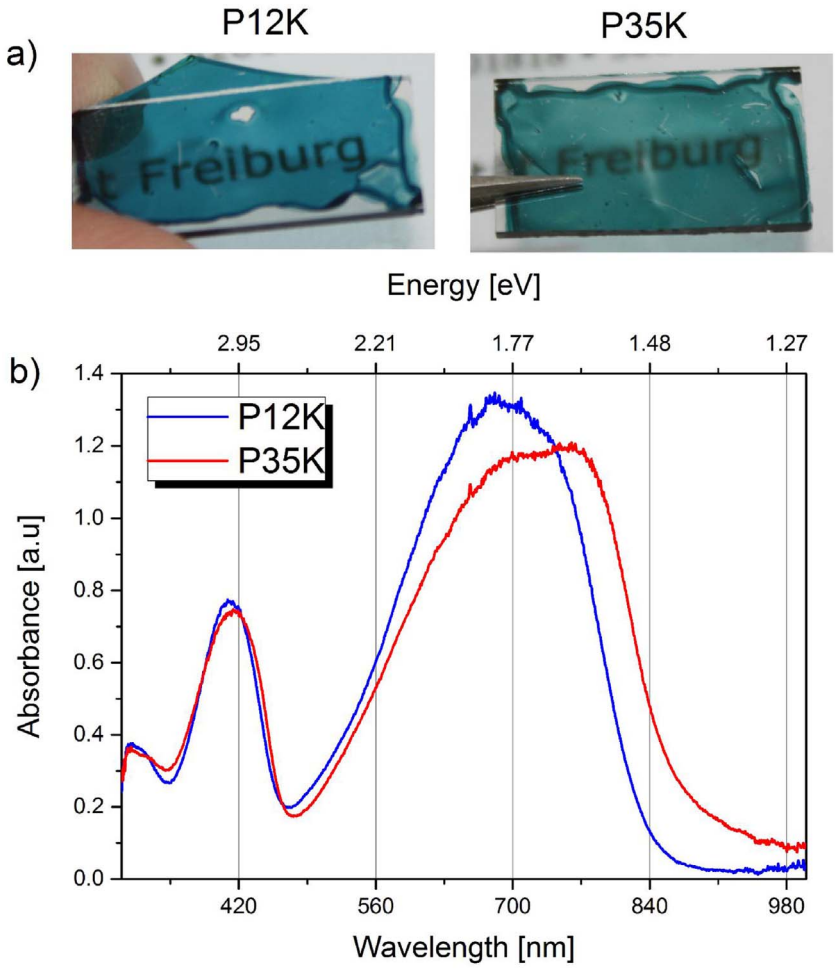

Fig. 1. Optical characteristics of P12K and P35K: (a) photograph of thin films spin coated on ITO covered glass, (b) absorption spectra of PCODTBT films on ITO-covered glass.

drying step at 3000 rpm, resulting in an active layer thickness of about 80 nm. In order to establish electrical contacts, an aluminum cathode layer was deposited by thermal evaporation. Afterwards, the devices were annealed at 145 °C for 5 min and stored in a glove box under nitrogen atmosphere without any further encapsulation.

2.4. Characterization techniques

Optical microscopy images were taken with a Leica 6000 DM microscope. UV–vis absorption measurement were performed by using a TIDAS 100 J&M diode-array spectrometer (Spectralytics, Aalen, Germany). Current density versus voltage (*J–V*) characteristics were taken by a Keithley 2400 source meter under 100 mW/cm^2 illumination of a AM1.5G xenon light source sun simulator (LOT-Oriel LSH102).

3. Results and discussion

Fig. 1 shows the optical properties of PCPDTBT films spin coated on ITO covered glass. The P12K solution appeared more blue compared to that P35K. The different color was more obvious after spin coating polymer films onto ITO substrates as shown in Fig. 1a. It was reported that the electrochemical band gap energy of PCPDTBT based on cyclic voltammetry measurements is estimated to be about 1.73 eV, and is slightly dependent on the polymer molecular weight [22]. In this work, the optical band gap energies were estimated from the onset of the absorption signal of the UV–vis spectra shown in Fig. 1, and were found to be about 1.48 eV and 1.43 eV for P12K and P35K respectively, which is consistent with results from literature [1,23–26]. Such a low band gap facilitates wide absorption into the visible wavelength range, which is preferred for solar cell applications in order to achieve high power conversion efficiencies [27,28]. The blue-shift which has been found in P12K suggests that it has lower crystallinity compared to that of higher-Mw P15K samples. A similar behavior also has been reported for thin films of P3HT [29], F8TBT [30] and MEH-PPV [31].

Initial experiments were performed to assess the influence of the molecular weight of the polymer on the HSCs device performance. Photovoltaic devices were prepared based on the design shown in Fig. 2a. The HOMO and LUMO level of PCPDTBT of −5.3 eV and −3.5 eV respectively were adopted from literature [1]. The valence and conduction band edges of CdSe are expected at about −5.59 eV and −3.62 eV respectively and referred to data for similarly-sized of CdSe [32].

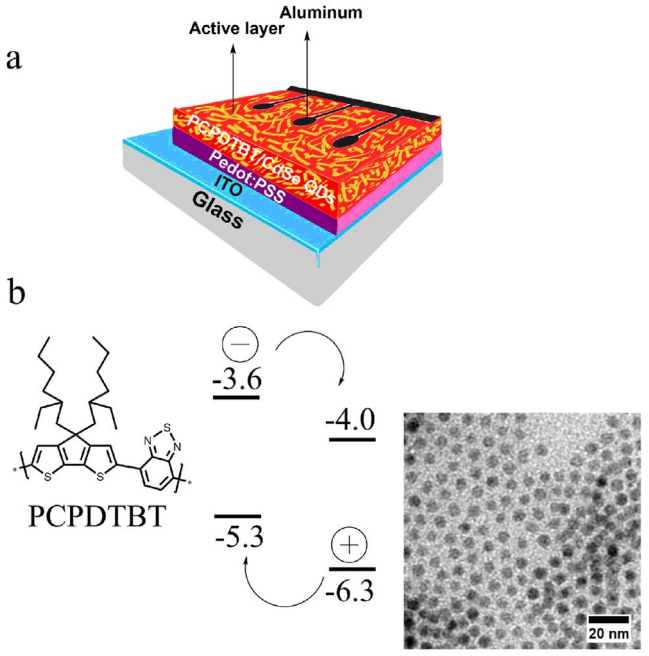

Fig. 2. (a) Schematic structure of a typical fabricated solar cell device, (b) chemical structure (left) and energy level diagram of PCPDTBT in comparison with CdSe QDs (middle), as well as a TEM image of CdSe QDs (right).

It is known that molecular weight can affect the physical characteristics of polymers [33–35]. High moleculer weight of polymer results generally in higher viscosity and poor processing ability [36,37]. In addition, it has been reported that polymer dissolution decreases with increased polymer molecular weight [38]. In order to investigate the influence of the molecular weight effect and the film annealing treatment on the morphology of the photoactive layer, images of photoactive layers before aluminum deposition were taken by optical microscopy as shown in Fig. 3. It can be observed from Fig. 3a and c that the initial morphology of P35K based active layer shows the appearance of many big black particles of probably undissolved polymer whereas P12K showed only a few aggregates with relatively small sizes. This shows that the two polymers have different solubility in chlorobenzene. Interestingly, after thermal annealing at 150 °C for 5 min, morphologies exhibited some changes. The number of aggregates which were found in P12K based device have been significantly decreased. A similar behavior was found for P35K based films, where the bigger aggregates have been minimized significantly too. The heat treatment during thermal annealing obviously helps the polymer to disperse.

Fig. 4 presents the absorption spectra of the optical absorption of spin-coated films of hexanoic acid treated-CdSe QDs/PCPDTBT (86:14 wt.%) with two different Mw for the polymer. The films were casted from chlorobenzene solutions onto PEDOT:PSS coated ITO, before and after thermal annealing for 5 min at 150 °C. The absorption maximum of the film casted from P12K solution is observed at a wavelength of 730 nm. A maximum at 768 nm is observed when the film is casted from P35K solution. The absorption band edge of the films casted from P12K and P35K solutions are observed at 853 and 871 nm, respectively. Contrary to the behavior of P3HT:PCBM which shows a redshift after annealing [39–45], the maximum absorption peak and absorption band edge were blue-shifted by ~10 and ~15 nm respectively after annealing. We suspect that the high percentage of three-dimensional CdSe nanostructures (86 wt.%) loaded in the blend film decreased the ordered internal structure of the PCPDTBT polymer chains. The peak at 635 nm in both spectra is caused by CdSe QDs. The inset of Fig. 4 displays a higher magnification of the respective CdSe QD absorption signals for both QD-polymer hybrid films. After comparing the ratios of the absorption maxima between the main peak (deriving from the polymer part) and the “CdSe QD” peak one can conclude an overall higher QD content for the P12K based hybrid film in comparison to the P35K based hybrid film.

The results displayed in Fig. 5 and summarized in Table 2 show the PCE values of differently composed hybrid solar cells directly after preparation, after annealing at 150 °C for 10 min and after one-week storage under nitrogen atmosphere. The low Mw P12K based devices exhibited an initial PCE values of 1.07 ± 0.27%, whereas an initial PCE of about 0.82 ± 0.06% was reached for P35K devices before annealing. After annealing treatment, both device types showed an increase in PCEs values, as a result of higher Jsc. P12K based devices exhibited an average PCE after annealing of about 1.94 ± 0.01%, whereas P35K based devices showed a PCE of 1.39 ± 0.13%. In other words, a PCE increase of 45% and 41% were achieved by annealing treatment in P12K and P35K respectively. Interestingly, after one-week storage under nitrogen atmosphere, the P12K based devices showed a remarkable stability in device performance. The PCE after one-week storage was found to be 1.86 ± 0.25% for P12K however, P35K based devices showed a significant drop in PCE down to 1.14 ± 0.23%. Simply, a decrease in PCE of 18% was recorded for high Mw P35K based devices, while low Mw P12K based devices showed only losses of 4%.

The values of R_{sh} and R_s can also be used to evaluate the device performance. It was reported that decreasing R_{sh} is usually

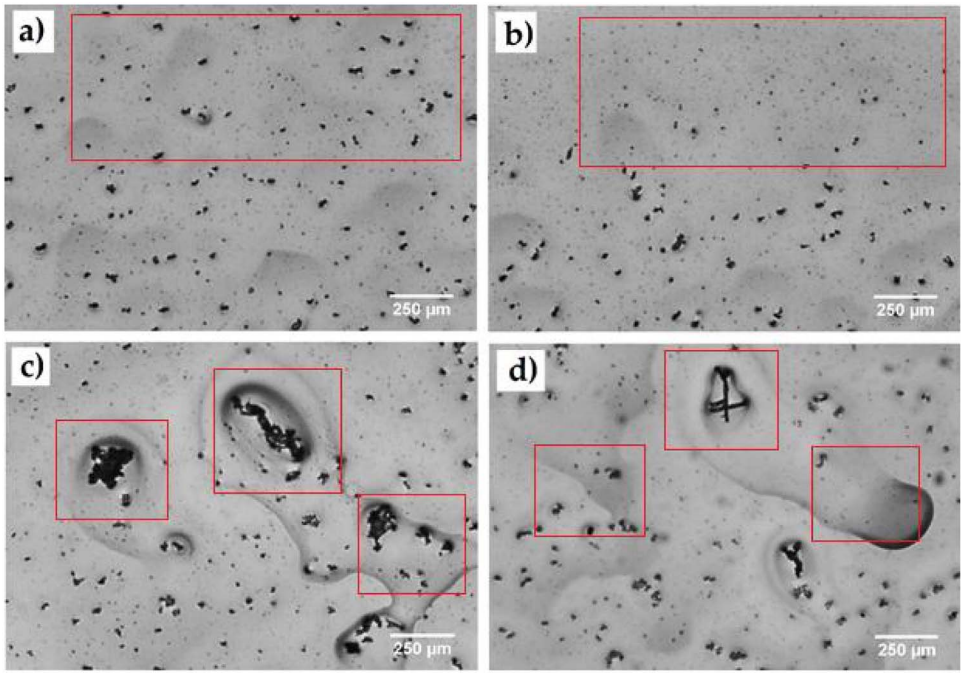

Fig. 3. Evolution of Morphology during annealing. P12K before (a) and after annealing treatment (b); P32K before (c) and after annealing treatment(d). Polymer was dispersed in chlorobenzene at 20 mg/mL The red-box shows the area of morphology changes due to annealing.

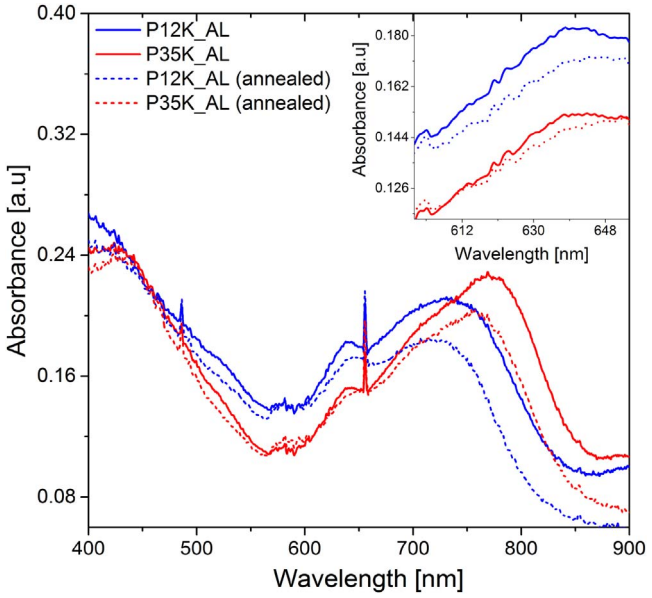

Fig. 4. Absorption spectra of PCPDTBT:CdSe QDs photoactive layer (14:86 wt.%) using P12K and P35K before and after thermal annealing at 150 °C for 5 min. Inset: stronger absorption signal of CdSe QDs appears in P12K. The strong narrow peak at about 660 nm is a peak from the spectrometer lamp.

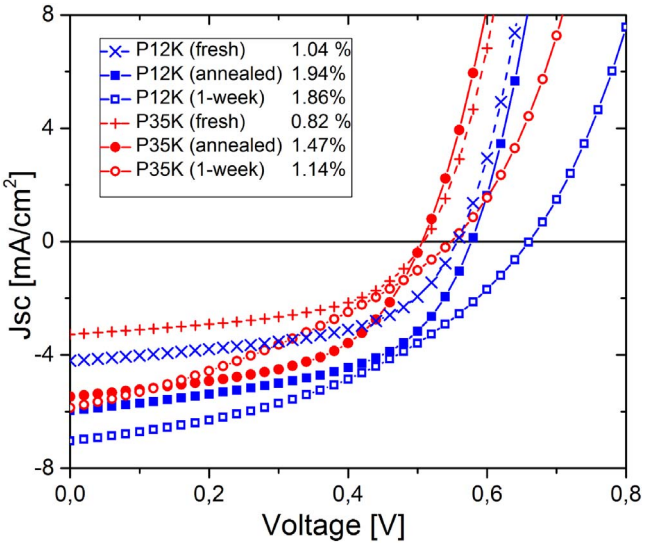

Fig. 5. Current density-voltage (J-V) characteristic of devices fabricated from two types of PCPDTB; high molecular weight (P35K) and low molecular weight (P12K), directly after device preparation, after annealing and after one-week storage under nitrogen atmosphere.

accompanied by an increasing R_s and vice versa [46–49]. Ideally, R_s should be the lower the better, and R_{sh} the higher the better. A high R_s reduces also J_{SC}; a low R_{sh} leaks off some current, leading to a loss in PCE. Contact resistance and charge recombination at the interface are two major reasons that lead to the increase of R_s and decrease of R_{sh} respectively [50]. Many reports have concluded that the increase in active layer mobilities are correlated with lower R_s values and, ultimately, higher cell efficiencies [51,52]. R_s is often the dominant parameter determining the fill factor (by altering the slope of the current density–voltage (J–V) curve near the V_{OC}) and is therefore of key importance for high-efficiency solar cells [53]. It can be observed in Fig. 6 that the initial values of the R_{sh} and R_s are fairly similar for both solar cell types. The effect of high R_{sh} values of both devices are resulting in high *FF* values, of 0.66 and 0.68 for P12K and P35K respectively.

However, slightly lower R_s in P12K has contributed to the higher short-circuit current. The lower performance of P35K based devices can be attributed to inherent properties of higher Mw polymer. Increasing Mw which is accompanied by an increase in the chain entanglements, will lead to higher viscosity [36,37]. Consequently, this will retard the CdSe QDs distribution in the hybrid system which can be seen by the lower signal absorption of CdSe ODs displayed in inset of Fig. 4. Furthermore, microscopy images of P12K based films has displayed better initial morphology compared to P35K based films (see Fig. 3a and c). It has been know that the tendency of a conjugated polymer material to aggregate is a key factor in controlling both the charge carrier mobility as well as the ability of excited states to dissociate when being in contact with an electron-accepting material [54]. Inhomogeneous distribution of CdSe QDs in the PCPDTBT matrix promotes insufficient charge separation and electron transport; thus reducing *Jsc*, *FF*, and the overall device efficiency. The better performance shown for low Mw PCPDTBT

Table 2
Summary of devices performance of both categories of solar cell devices by P12K and P35K PCPDTBT as polymer. For each polymer three different solar cells were measured.

PCPDTBT	Voc [V]	Jsc[mA/cm2]	FF	PCE [%]	Rsh [Ω.cm^2]	Rs [Ω.cm^2]	Decrease in PCE [%]
P12 K (fresh)	0.55 ± 0.02	3.70 ± 0.74	0.66 ± 0.02	1.07 ± 0.27	593	15.1	
P12 K (annealed)	0.57 ± 0.01	6.66 ± 0.16	0.56 ± 0.00	1.94 ± 0.01	625	13.1	3.89
P12 K (1-week)	0.65 ± 0.01	6.77 ± 0.59	0.42 ± 0.01	1.86 ± 0.25	592	23.4	
P35 K (fresh)	0.51 ± 0.01	3.09 ± 0.22	0.68 ± 0.01	0.82 ± 0.06	579	16.0	
P35 K (annealed)	0.51 ± 0.01	5.16 ± 0.04	0.61 ± 0.01	1.39 ± 0.13	600	15.6	17.98
P35K(1-week)	0.50 ± 0.08	5.73 ± 1.22	0.35 ± 0.02	1.14 ± 0.23	336	34.7	

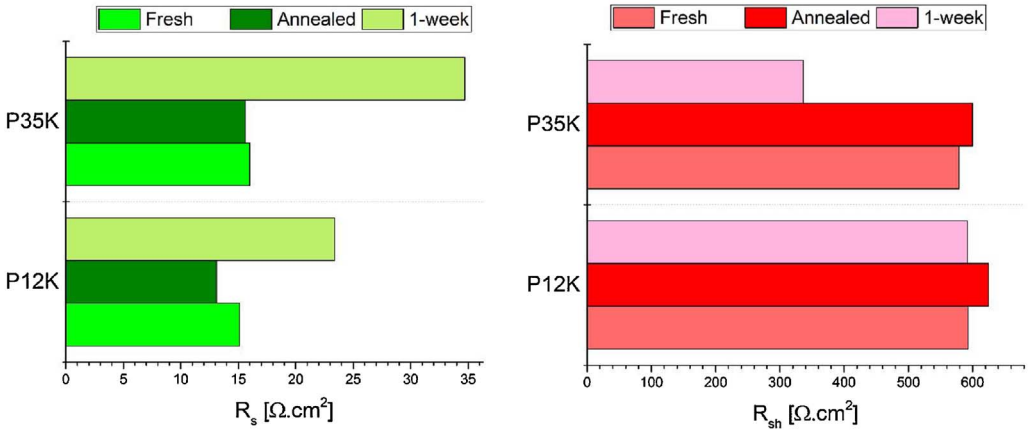

Fig. 6. Summary of absolute values of specific shunt resistances (R_{sh}) (left) and specific series resistances (R_s) (right) for CdSe QD/PCPDTBT hybrid solar cells with two different molecular weights, P12K and P15K for PCPDTBT respectively.

in such polymer/CdSe QDs hybrid solar cells is also in agreement with other results which reported that the low Mw polymer has strong impact on the improvement of the nanoscale phase separation [25,55,56].

The initial morphology of spin-coated films is the result of a kinetically frozen phase separation or crystallization and far from a morphology at thermodynamically equilibrium [57–60]. Therefore, there is likely a strong thermodynamic driving force for the samples to reorganize toward the equilibrium state, which can be accelerated during annealing [61]. After annealing treatment, both types of devices showed a decrease in R_s. P12K based devices were found to have lower values for R_s which is resulting in higher values of *Jsc* compared to P35K, and therefore leads to the higher PCE. The increasing PCE values strongly indicate that annealing treatment which is accompanied by morphology changes (see Fig. 3b and d) could improve hybrid solar cells performance. Firstly, annealing facilitates CdSe QDs to distribute into the polymer matrix resulting into better interfacial donor acceptor contacts and improving the contact with the Al electrode [2,57,62]. Secondly, it allows the removal of CdSe QDs ligands, which leads to a decrease of distances between nanoparticles and, in turn increases the CdSe QDs packing densities, thereby improving the electrical conductivity within the active layer [63,64].

After one-week storage under nitrogen atmosphere without any further encapsulation, low Mw P12K based solar cell devices showed a better preservation of device performance compared to that P35K. Compared to that annealed values, the increasing R_s and decreasing R_{sh} after one-week of storage for P35K devices are striking. A decrease in R_{sh} of about 44% has been obtained for P35K devices whereas for P12K devices only showed a decrease of about 5.3%. P35K devices displayed a 2.2-fold increase in R_s while P12K devices showed a 1.8-fold increase in R_s. We propose that annealing treatment of low Mw PCPDTBT facilitates the polymer chains to arrange into thermodynamically more stable film structures due to a better distribution of CdSe QDs within the photoactive layer blend, which leads to a general morphology stabilization. Thus would allow the optimized photoactive layer morphology to be “locked” and would decrease the tendency of the blend to phase segregate over time [65–67]. Further experiments are needed to monitor hybrid film morphology changes over time proving this assumption, which are planned to be performed in near future. This results are important for making high efficiency hybrid solar cells with long-term stability. Recent developments revealed that blend optimization, QD surface modification, and incorporation of nanocarbon structures into PCPDTBT/CdSe QDs active layer, have boosted the efficiencies above 4% accompanied with an increase of device stability over time which are important issues for further device developments needed to reach a potential commercialization [4].

4. Summary and conclusion

In conclusion, high efficient, stable, BHJ hybrid solar cells fabricated with two different molecular weight PCPDTBT, which act as the electron donor, have been demonstrated. The best performance was obtained with low molecular weight of PCPDTBT/CdSe QDs, where power conversion efficiencies of approximately 2% are demonstrated. The short annealing treatment affected the morphology and has been found to improve the device performance. Moreover, about 96% of the original PCE remained after storage under nitrogen protection for one-week storage in a glove-box without any further encapsulation. The stability of hybrid solar cells can be correlated to an optimized donor-acceptor nanomorphology, leading to inhibit the degradation process within the photoactive layer. Our results indicate that the use of low molecular weight PCPDTBT polymer is a promising pathway for the fabrication of high efficient hybrid solar cells with improved long-term stability of device performance.

Acknowledgement

We gratefully acknowledge the Indonesian Directorate General of Higher Education (DIKTI) High Achiever Scholarship 2012–2015.

References

[1] D. Mühlbacher, M. Scharber, M. Morana, et al., High photovoltaic performance of a low-bandgap polymer, Adv. Mater. 18 (21) (2006) 2884–2889.
[2] Y. Zhou, M. Eck, C. Veit, et al., Efficiency enhancement for bulk-heterojunction hybrid solar cells based on acid treated CdSe quantum dots and low bandgap

polymer PCPDTBT, Sol. Energy Mater. Sol. Cells 95 (4) (2011) 1232–1237.
[3] Y. Sun, J.H. Seo, C.J. Takacs, et al., Inverted polymer solar cells integrated with a low-temperature-annealed sol-gel-derived ZnO film as an electron transport layer, Adv. Mater. 23 (14) (2011) 1679–1683.
[4] M. Eck, C. van Pham, S. Zufle, et al., Improved efficiency of bulk heterojunction hybrid solar cells by utilizing CdSe quantum dot-graphene nanocomposites, Phys. Chem. Chem. Phys. 16 (24) (2014) 12251–12260.
[5] Z. He, C. Zhong, X. Huang, et al., Simultaneous enhancement of open-circuit voltage, short-Circuit current density, and fill factor in polymer solar cells, Adv. Mater. 23 (40) (2011) 4636–4643.
[6] Y.W. Soon, H. Cho, J. Low, et al., Correlating triplet yield, singlet oxygen generation and photochemical stability in polymer/fullerene blend films, Chem. Commun. 49 (13) (2013) 1291–1293.
[7] B.R. Aïch, J. Lu, S. Beaupré, et al., Control of the active layer nanomorphology by using co-additives towards high-performance bulk heterojunction solar cells, Org. Electron. 13 (9) (2012) 1736–1741.
[8] H.-C. Liao, C.-C. Ho, C.-Y. Chang, et al., Additives for morphology control in high-efficiency organic solar cells, Mater. Today 16 (9) (2013) 326–336.
[9] F. Liu, Y. Gu, X. Shen, et al., Characterization of the morphology of solution-processed bulk heterojunction organic photovoltaics: topical issue on Conductive Polymers, Prog. Polym. Sci. 38 (12) (2013) 1990–2052.
[10] M. Krueger, M. Eck, Y. Zhou, et al., Semiconducting Nanocrystal/Conjugated polymer composites for applications in hybrid polymer solar cells, Semiconducting Polymer Composites, Wiley-VCH Verlag GmbH & Co. KGaA, 2012, pp. 361–397.
[11] Yunfei Zhou, Bulk-Heterojunction Hybrid Solar Cells Based on Colloidal CdSe Quantum Dots and Conjugated Polymers, Dissertation, University of Freiburg, 2011 (20/02/2011).
[12] Yunfei Zhou, Michael Eck, Michael Krüger, Organic-inorganic hybrid solar cells: state of the art, challenges and perspectives, in: Leonid A. Kosyachenko (Ed.), Solar Cells − New Aspects and Solutions, In Tech, 2011, pp. 95–120.
[13] Y. Zhou, M. Eck, M. Kruger, Bulk-heterojunction hybrid solar cells based on colloidal nanocrystals and conjugated polymers, Energy Environ. Sci. 3 (12) (2010) 1851–1864.
[14] Y. Zhou, M. Eck, C. Men, et al., Efficient polymer nanocrystal hybrid solar cells by improved nanocrystal composition, Sol. Energy Mater. Sol. Cells 95 (12) (2011) 3227–3232.
[15] Y. Zhou, F.S. Riehle, Y. Yuan, et al., Improved efficiency of hybrid solar cells based on non-ligand-exchanged CdSe quantum dots and poly(3-hexylthiophene), Appl. Phys. Lett. 96 (1) (2010) 133041–133044.
[16] X. Yang, J. Loos, S.C. Veenstra, et al., Nanoscale morphology of high-performance polymer solar cells, Nano Lett. 5 (4) (2005) 579–583.
[17] I. Gur, N.A. Fromer, C.-P. Chen, et al., Hybrid solar cells with prescribed nanoscale morphologies based on hyperbranched semiconductor nanocrystals, Nano Lett. 7 (2) (2007) 409–414.
[18] A.M. Ballantyne, L. Chen, J. Dane, et al., The effect of poly(3-hexylthiophene) molecular weight on charge transport and the performance of polymer:fullerene solar cells, Adv. Funct. Mater. 18 (16) (2008) 2373–2380.
[19] W. Ma, J.Y. Kim, K. Lee, et al., Effect of the molecular weight of poly(3-hexylthiophene) on the morphology and performance of polymer bulk heterojunction solar cells, Macromol. Rapid Commun. 28 (17) (2007) 1776–1780.
[20] A.F. Madsuha, C. van Pham, M. Krueger, Thiolated carbon Nanotubes/CdSe quantum dot based hybrid solar cells with improved long-term stability, Nano Hybrids 9 (2016) 7–14.
[21] Y. Yuan, F.-S. Riehle, H. Gu, et al., Critical parameters for the scale-up synthesis of quantum dots, J. Nanosci. Nanotechnol. 10 (9) (2010) 6041–6045.
[22] D. Mühlbacher, M. Scharber, M. Morana, et al., High photovoltaic performance of a low-bandgap polymer, Adv. Mater. 18 (21) (2006) 2884–2889.
[23] S. Dayal, N. Kopidakis, D.C. Olson, et al., Photovoltaic devices with a low band gap polymer and CdSe nanostructures exceeding 3% efficiency, Nano Lett. 10 (1) (2010) 239–242.
[24] G. Li, R. Zhu, Y. Yang, Polymer solar cells, Nat Photon 6 (3) (2012) 153–161.
[25] C. Soci, I.-W. Hwang, D. Moses, et al., Photoconductivity of a low-bandgap conjugated polymer, Adv. Funct. Mater. 17 (4) (2007) 632–636.
[26] I.-W. Hwang, C. Soci, D. Moses, et al., Ultrafast electron transfer and decay dynamics in a small band gap bulk heterojunction material, Adv. Mater. 19 (17) (2007) 2307–2312.
[27] C.J. Brabec, C. Winder, N.S. Sariciftci, et al., A low-Bandgap semiconducting polymer for photovoltaic devices and infrared emitting diodes, Adv. Funct. Mater. 12 (10) (2002) 709–712.
[28] J.Y. Kim, K. Lee, N.E. Coates, et al., Efficient tandem polymer solar cells fabricated by all-solution processing, Science 317 (5835) (2007) 222–225.
[29] T.C. Monson, M.T. Lloyd, D.C. Olson, et al., Photocurrent enhancement in polythiophene- and alkanethiol-modified ZnO solar cells, Adv. Mater. 20 (24) (2008) 4755–4759.
[30] C. Müller, E. Wang, L.M. Andersson, et al., Influence of molecular weight on the performance of organic solar cells based on a fluorene derivative, Adv. Funct. Mater. 20 (13) (2010) 2124–2131.
[31] K. Koynov, A. Bahtiar, T. Ahn, et al., Molecular weight dependence of chain orientation and optical constants of thin films of the conjugated polymer MEH-PPV, Macromolecules 39 (25) (2006) 8692–8698.
[32] C. Querner, P. Reiss, S. Sadki, et al., Size and ligand effects on the electrochemical and spectroelectrochemical responses of CdSe nanocrystals, Phys. Chem. Chem. Phys. 7 (17) (2005) 3204–3209.
[33] L.F. Boesel, S. LeMeur, L. Thöny-Meyer, et al., The effect of molecular weight on the material properties of biosynthesized poly(4-hydroxybutyrate), Special Issue: Biodegradable Biopolymers 71 (2014) 124–130.
[34] W.G. Perkins, N.J. Capiati, R.S. Porter, The effect of molecular weight on the physical and mechanical properties of ultra-drawn high density polyethylene, Polym. Eng. Sci. 16 (3) (1976) 200–203.
[35] J.R. Martin, J.F. Johnson, A.R. Cooper, Mechanical properties of polymers: the influence of molecular weight and molecular weight distribution, J. Macromol. Sci. Part C 8 (1) (1972) 57–199.
[36] H. Ha, S.C. Kim, K. Ha, Effect of molecular weight of polymer matrix on the dispersion of MWNTs in HDPE/MWNT and PC/MWNT composites, Macromol. Res. 18 (5) (2010) 512–518.
[37] W.-F. Su, Polymer size and polymer solutions, in: W.-F. Su (Ed.), Principles of Polymer Design and Synthesis, Springer Berlin Heidelberg, Berlin, Heidelberg, 2013, pp. 9–26.
[38] B.A. Miller-Chou, J.L. Koenig, A review of polymer dissolution, Prog. Polym. Sci. 28 (8) (2003) 1223–1270.
[39] M. Al-Ibrahim, O. Ambacher, S. Sensfuss, et al., Effects of solvent and annealing on the improved performance of solar cells based on poly(3-hexylthiophene): Fullerene, Appl. Phys. Lett. 86 (20) (2005) 201120.
[40] H. Chen, Y.-C. Hsiao, B. Hu, et al., Tuning the morphology and performance of low bandgap polymer:fullerene heterojunctions via solvent annealing in selective solvents, Adv. Funct. Mater. 24 (32) (2014) 5129–5136.
[41] G. Li, V. Shrotriya, Y. Yao, et al., Investigation of annealing effects and film thickness dependence of polymer solar cells based on poly(3-hexylthiophene), J. Appl. Phys. 98 (4) (2005) 43704.
[42] H. Chen, Y.-C. Hsiao, B. Hu, et al., Control of morphology and function of low band gap polymer-bis-fullerene mixed heterojunctions in organic photovoltaics with selective solvent vapor annealing, J. Mater. Chem. A 2 (25) (2014) 9883–9890.
[43] K.F. Jeltsch, M. Schädel, J.-B. Bonekamp, et al., Efficiency enhanced hybrid solar cells using a blend of quantum dots and nanorods, Adv. Funct. Mater. 22 (2) (2012) 397–404.
[44] F. Piersimoni, G. Degutis, S. Bertho, et al., Influence of fullerene photodimerization on the PCBM crystallization in polymer: fullerene bulk heterojunctions under thermal stress, J. Polym. Sci. B: Polym. Phys. 51 (16) (2013) 1209–1214.
[45] U. Zhokhavets, T. Erb, G. Gobsch, et al., Relation between absorption and crystallinity of poly(3-hexylthiophene)/fullerene films for plastic solar cells, Chem. Phys. Lett. 6 (2006) 347–350.
[46] K. Wang, Y. Zheng, G. Xu, et al., The inverse correlation between series resistance and parallel resistance of small molecule organic solar cells, Prog. Nat. Sci.: Mater. Int. 25 (4) (2015) 323–326.
[47] T.L. Chen, J.J.-A. Chen, L. Catane, et al., Fully solution processed p-i-n organic solar cells with an industrial pigment −Quinacridone, Org. Electron. 12 (7) (2011) 1126–1131.
[48] M.T. Lloyd, A.C. Mayer, A.S. Tayi, et al., Photovoltaic cells from a soluble pentacene derivative, Org. Electron. 7 (5) (2006) 243–248.
[49] M. Rusu, S. Wiesner, I. Lauermann, et al., Formation of charge-selective Mg–Ag electrodes to CuPc:C60 blend layers, Appl. Phys. Lett. 97 (7) (2010) 73504.
[50] A. Moliton, J.-M. Nunzi, How to model the behaviour of organic photovoltaic cells, Polym. Int. 55 (6) (2006) 583–600.
[51] S.M. Sze, K.K. Ng, p-n junctions, Physics of Semiconductor Devices, John Wiley & Sons, Inc, 2006, pp. 77–133.
[52] J. Xue, S. Uchida, B.P. Rand, et al., 4.2% efficient organic photovoltaic cells with low series resistances, Appl. Phys. Lett. 84 (16) (2004) 3013–3015.
[53] J.D. Servaites, S. Yeganeh, T.J. Marks, et al., Efficiency enhancement in organic photovoltaic cells: consequences of optimizing series resistance, Adv. Funct. Mater. 20 (1) (2010) 97–104.
[54] L. Li, G. Lu, X. Yang, Improving performance of polymer photovoltaic devices using an annealing-free approach via construction of ordered aggregates in solution, J. Mater. Chem. 18 (17) (2008) 1984–1990.
[55] J. Kettle, M. Horie, L.A. Majewski, et al., Optimisation of PCPDTBT solar cells using polymer synthesis with suzuki coupling, photovoltaics, solar energy materials & thin films, IMRC 2009-Cancun 95 (8) (2011) 2186–2193.
[56] Z. Zhu, D. Waller, R. Gaudiana, et al., Panchromatic conjugated polymers containing alternating donor/acceptor units for photovoltaic applications, Macromolecules 40 (6) (2007) 1981–1986.
[57] C. Du, Y. Ji, J. Xue, et al., Morphology and performance of polymer solar cell characterized by DPD simulation and graph theory, Sci. Rep. 5 (2015) 16854 EP.
[58] A.J. Moulé, K. Meerholz, Controlling morphology in polymer–fullerene mixtures, Adv. Mater. 20 (2) (2008) 240–245.
[59] B.C. Thompson, J.M.J. Fréchet, Polymer–fullerene composite solar cells, Angew. Chem. Int. Ed. 47 (1) (2008) 58–77.
[60] X. Yang, J. Loos, Toward high-performance polymer solar cells: the importance of morphology control, Macromolecules 40 (5) (2007) 1353–1362.
[61] B.A. Collins, F.A. Bokel, D.M. DeLongchamp, Organic photovoltaic morphology, Organic Photovoltaics, Wiley-VCH Verlag GmbH & Co. KGaA, 2014, pp. 377–420.
[62] W. Ma, C. Yang, X. Gong, et al., Thermally stable, efficient polymer solar cells with nanoscale control of the interpenetrating network morphology, Adv. Funct. Mater. 15 (10) (2005) 1617–1622.
[63] U. Zhokhavets, T. Erb, G. Gobsch, et al., Relation between absorption and crystallinity of poly(3-hexylthiophene)/fullerene films for plastic solar cells, Chem. Phys. Lett. 6 (2006) 347–350.
[64] F. Tan, S. Qu, J. Wu, et al., Preparation of SnS2 colloidal quantum dots and their application in organic/inorganic hybrid solar cells, Nanoscale Res. Lett. 6 (1) (2011) 1–8.
[65] J.W. Rumer, I. McCulloch, Organic photovoltaics: crosslinking for optimal morphology and stability, Mater. Today 18 (8) (2015) 425–435.
[66] B.C. Schroeder, Z. Li, M.A. Brady, et al., Enhancing fullerene-Based solar cell lifetimes by addition of a fullerene dumbbell, Angew. Chem. Int. Ed. 53 (47) (2014) 12870–12875.
[67] J.U. Lee, J.W. Jung, J.W. Jo, et al., Degradation and stability of polymer-based solar cells, J. Mater. Chem. 22 (46) (2012) 24265–24283.